KeAi
CHINESE ROOTS
GLOBAL IMPACT

Available online at www.sciencedirect.com

ScienceDirect

Green Energy & Environment 8 (2023) 194–199

www.keaipublishing.com/gee

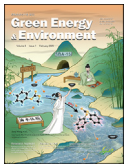

Research paper

Visible-light degradation of azo dyes by imine-linked covalent organic frameworks

Hongbo Xue, Sen Xiong, Kai Mi, Yong Wang*

State Key Laboratory of Materials-Oriented Chemical Engineering, And College of Chemical Engineering, Nanjing Tech University, Nanjing, 211816, Jiangsu, China

Received 30 June 2020; revised 15 August 2020; accepted 20 September 2020
Available online 25 March 2021

Abstract

Covalent organic frameworks (COFs) are nanoporous crystalline polymers with densely conjugated structures. This work discovers that imine-linked COFs exhibit remarkable photodegradation efficiency to azo dyes dissolved in water. Visible light generates different types of radicals from COFs, and superoxide radicals break N═N bonds in dye molecules, resulting in 100% degradation of azo dyes within 1 h. In contrast, these dyes cannot be degraded by conventionally used photocatalysts, for example, TiO_2. Importantly, the COF photocatalysts can be recovered from the dye solutions and re-used to degrade azo dyes for multiple times without loss of degradation efficiency. This work provides an efficient strategy to degrade synthetic dyes, and we expect that COFs with designable structures may use as new photocatalysts for other important applications.

Keywords: Covalent organic frameworks; Dyes; Photocatalytic degradation; Porous polymer; Water pollution

1. Introduction

Dye-containing wastewaters from textile and printing industries are significant threatens to environment and eco-biology because of the toxicity, non-biodegradability and potential carcinogenic nature of artificial dyes [1–3]. A number of measurements have been taken to clean up dyes from water, such as adsorption, flocculation and biological treatments [4,5]. However, there are some inevitable shortcomings of these methods [6–9].

Comparing with other methods, photocatalysis has received extensive attention for its potential to degrade dyes with low energy consumption [10]. Conventional photocatalysts, such as zinc oxide (ZnO) and titanium dioxide (TiO_2) [11], have shown decent performance in degradation of a certain number of dyes, including squarylium cyanine (SQ), acid orange 7 (AC7) and reactive red 198 (RR198) [12–14]. To enhance the contact between the metal oxide catalysts and the target dye pollutants, stirring is usually required, which adds extra expense to the photocatalytic process [11]. In addition, metal-complex dyes, which complex with metal ions and inactivate the catalysts, cannot be degraded by these metal oxide catalysts [15–18]. Therefore, new catalysts are urgently required to solve these problems.

Covalent organic frameworks (COFs) are a group of porous crystalline polymers with low density, programmable chemical structures and large surface area [19,20]. COFs have shown potential applications in many fields, such as adsorption, catalysis, and membrane separations [21]. Due to their unique structures and electrical properties, COFs have also been used in photocatalysis [22]. COFs have shown good photocatalytic performance for the *E* to *Z* isomerization of alkenes [23]. Also, COFs have recently been applied as metal-free visible-light photocatalyst for CO_2 reduction and hydrogen generation

* Corresponding author. Fax: +86 25-83172292.
E-mail address: yongwang@njtech.edu.cn (Y. Wang).

https://doi.org/10.1016/j.gee.2020.09.010

[24,25]. Smaller particle size and lower density which is close to water, make COFs highly dispersible in water to enhance photocatalysis. Moreover, metal-free COFs may solve the predicament that metal-complex dyes cannot be effectively degraded by typical metal oxide catalysts. Based on these considerations, we expect that COFs could be employed as new photocatalysts for dye degradation. Due to high chemical stability and water tolerance, imine-linked COFs can deliver their functions in aqueous solutions [26]. Moreover, imine-linked COFs with densely π-conjugation units are expected to promote photo-induced electrons separation and charge transport, which are highly desired in photocatalysis.

In this work, we synthesize two extensively used imine-linked COFs, TpBD and TpPa, to investigate their photocatalytic degradation efficiency on dyes. TpBD and TpPa were synthesized by Schiff-based reactions with 2,4,6-triformylphloroglucinol (Tp) and diamines.

2. Experimental section

2.1. Materials

All reagents were used as received without further purification. 2,4,6-triformylphloroglucinol (Tp, 98%, Yanshen Technology Co., Ltd.), *p*-phenylenediamine (Pa, 97%, Aladdin) and benzidine (BD, 95%, Aladdin) were used as monomers. Eriochrome black T (EBT, Aladdin), eriochrome black A (EBA, TCI), mordant black 17 (MB17, Macklin), mordant black 3 (MB3, Yuanye) and mordant red 7 (MR7, Yuanye) were employed as model dyes (Fig. S1). Titanium dioxide (TiO_2, 99.8%) was supplied by Macklin. *p*-benzoquinone (BQ, 98%) was supplied by Hushi. Ethylenediaminetetraacetic acid disodium salt (EDTA-2Na, 99.95%) was bought from Institute of Chemical Reagent. 2,2,6,6-tetramethyi-1-piperidinyloxy (TEMPO, 97%) was purchased from Accela ChemBio Co., Ltd. 1,3,5-trimethylbenzene (97%), 1,4-dioxane (99%), ethanol (99.8%), acetone (99.5%), acetic acid (Ac, 99%) and *tert*-Butanol (tB, 98%) were bought from local suppliers. Deionized water was from Wahaha Group Co., Ltd.

2.2. Characterization

The Fourier transform infrared spectroscopy (FT-IR, Nicolet 8700, Thermo Fisher Scientific) was used to analyze the chemical structures of the monomers and COFs. Powder X-ray diffraction (XRD, Rigaku SmartLab) was used to analyze the crystallinity of COFs. The measurements were conducted at room temperature with 2θ ranging from 0.5° to 30° and a scanning rate of 0.02° s^{-1}. Morphologies of the COFs were characterized by a field-emission scanning electron microscope (FE-SEM, Hitachi S-4800) at the accelerating voltage of 5 kV. Prior to the test, a thin layer of gold was sputter-coated onto the sample to enhance the conductivity. UV-visible absorption spectrometer (UV-vis, NanoDrop 2000c, Thermo Fisher Scientific) was employed to determine the variations of dye concentrations. UV-visible-near-infrared diffuse reflectance spectrophotometer (UV-vis-NIR DRS, Shimazu UV-3600) was used to analyze the energy gaps and absorbance edges of catalysts in a wavelength from 300 nm to 700 nm. After photocatalytic degradation, the COFs powders were separated from the mixture, and the photocatalytic degradation products were investigated by Raman Spectra (Reinshaw Invia Reflex) with a laser emitting of 532 nm in liquid state. Active radicals were investigated by electron paramagnetic resonance (EPR, Bruker A300).

2.3. Synthetic procedures

TpBD: To a pyrex tube (o.d. × i.d. = 10 × 8 mm^2 and length 25 cm), Tp (0.3 mmol, 63 mg), BD (0.45 mmol, 83 mg), 1,3,5-trimethylbenzene (1.5 mL), 1,4-dioxane (1.5 mL) and 6 mol L^{-1} acetic acid (0.5 mL) were added in sequence. The mixture was sonicated for 10 min to obtain a well-dispersed solution. Afterwards, the tube was flash frozen in liquid nitrogen, degassed by three freeze–pump–thaw cycles and flame sealed off under vacuum. The tube was then heated at 120 °C for 3 days. After reaction, the product was collected by filtration, thoroughly washed with acetone (50 mL) and ethanol (250 mL), respectively. The collected product was further dried at 120 °C under vacuum for 24 h to afford yellow powders with a total yield of 74% (108 mg). Synthesis procedure of TpPa was similar to TpBD, but using Pa (0.45 mmol, 48 mg) as a monomer. The TpPa was obtained as dark red powders with a yield of 83% (92 mg).

3. Results and discussion

3.1. Characterization of TpBD

Fourier transform infrared spectrometer (FTIR) (Fig. S2) evidences the monomers were reacted with each other, leading to the corresponding COFs underwent enol–keto tautomerism [27]. X-ray diffraction (XRD) patterns reveal that the synthesized TpBD exhibit good crystallinity. As shown in Fig. 1a, the characteristic peaks in XRD pattern of experimental TpBD is consistent with that of simulation. The first peak at 3.38°, corresponding to the (100) reflection plane of TpBD, indicating the formation of regular channel structure [28]. The broad peak at 27.28° originated from the (001) plane confirms the π-conjugation between COF layers [27]. Ordered π-π stacking is significant for electron transfer during photocatalysis.

It is known that the ultraviolet occupies only 8% of the sunlight, while the visible light holds 43% of it [29]. As shown in Fig. 1b, UV-visible-near-infrared diffuse reflectance spectrophotometer (UV-vis-NIR DRS) spectrum showed that TpBD exhibited excellent light-harvesting capability which spanned both the ultraviolet and the visible-light region. Moreover, TpBD showed an absorption edge adjacent to 600 nm, implying that it could take better utilization of solar energy, whose absorption edge is 320 nm [11]. We then determine the optical band gap energy (E_g) from the Kubelka–Munk function (Eq. (1)): [30].

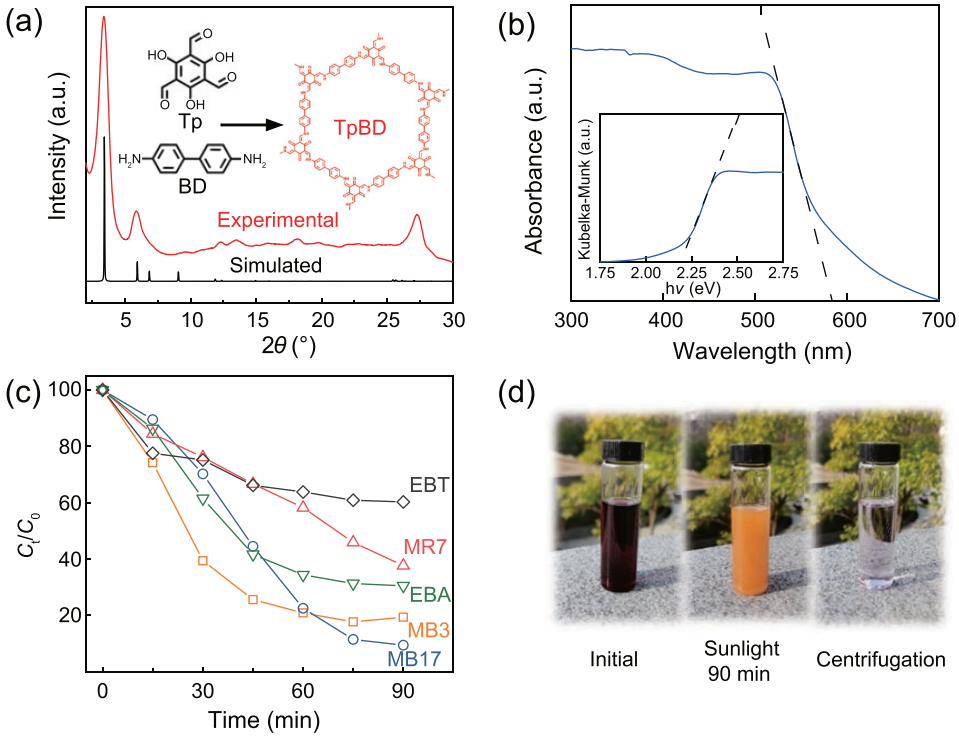

Fig. 1. (a) XRD patterns of TpBD. (b) DRS spectrum of TpBD. Insert: E_g of TpBD determined from Kubelka–Munk function. (c) Photocatalytic degradation of dyes under visible light with TpBD. (d) Photographs of MB17 aqueous solution mixed with TpBD for photocatalytic degradation under natural sunlight.

$$(\alpha h\upsilon)^{n/2} = \mathrm{A}\left(h\upsilon - E_g\right) \quad (1)$$

where α represents the absorption coefficient, $h\upsilon$ is the photon energy, n is the power index determined by the type of optical transition, A is a constant and E_g is the band gap energy. Optical band gap energy of TpBD was determined to be 2.19 eV by Tauc plot. Such a low E_g means the better utilization of sunlight during the photocatalytic degradation.

3.2. Visible-light degradation

We then examine the visible-light photocatalytic degradation efficiency of TpBD with typical TiO_2 particles as the control for comparison. High concentration solutions of azo dyes are purposely used to simulate the textile and printing industry wastewaters as targets for visible-light degradation. In order to eliminate the effect of adsorption, the catalyst and dye solution were pre-mixed and stored in dark for 60 min before light irradiation. Due to the excellent dispersibility, TpBD could blend with dye solutions easily without any stirring while TiO_2 required stirring for adequate mixing. As shown in Fig. S3, TiO_2 could hardly degraded mordant black 3 (MB3) and mordant black 17 (MB17). Only 4.6% of mordant red 7 (MR7), 9.0% of eriochrome black A (EBA) and 19.0% of eriochrome black T (EBT) can be degraded by TiO_2. After mixing with TiO_2, the maximum absorption increased and wavelength of the dye solutions became red-shifted. This abnormal phenomenon should be attributed to the complexation of dye molecules with TiO_2 [15–18]. After 90 min of exposure to visible light, 80.6% of MB3, 90.6% of MB17, 62.3% of MR7, 69.5% of EBA, and 39.8% of EBT were degraded (Fig. 1c). It is worth noting that all dyes are in high concentration ($\geq$100 mg L^{-1}) to highlight the photocatalytic ability of COFs.

We also used the natural sunlight as the light source to conduct the degradation test (Fig. 1d). Surprisingly, natural photocatalytic degradation efficiency was even better than that with stimulated light. Adding TpBD into the MB17 solution caused no obvious colour change. Under sunlight irradiation for 90 min, the solution faded, and the colour changed from original bluish violet into yellow which is the colour of TpBD. After centrifugation, the initial MB17 solution became clear and transparent, meaning that the solution with concentration of 150 mg L^{-1} was totally degraded by TpBD within 1 h. However, TiO_2 could hardly degraded MB17, only 18% of MB17 was degraded in 1 h with the same condition. This result could be attributed to the higher outside temperature (31 °C), which enhanced degradation [31]. As shown in Table S1, compared to other photocatalysts (organic, inorganic, or doped), TpBD shows better photocatalytic performance with a lower dosage, higher dye concentration, and less time. Of note, COFs are used without additional energy consumption for stirring.

MB17 was employed to investigate the kinetic behaviour of TpBD during the photocatalytic degradation. Calculation details were shown in Supporting Information. As shown in Table S2, the photocatalytic degradation process of TpBD fitted the first kinetic equation better, indicating that the rate of

photodegradation is proportional to the concentration of dye solution.

3.3. Photocatalytic degradation mechanism

In order to identify the degradation products, Raman spectra was employed to study the degradation of MB17. As shown in Fig. 2a, the band at 1102 cm^{-1} indicates the symmetric stretching vibration of $-SO_3$ group. The stretching of N=N chromophore appears at 1336 cm^{-1}, and the in-plane-bending vibration of hydroxyl is shown at 1445 cm^{-1}. The bond at 1603 cm^{-1} is mainly due to C–C asymmetric and symmetric stretching vibrations of naphthalene rings. In contrast, the spectrum of the degraded MB17 is quite different from the original one. Several domain bonds, including N=N bonds and part of OH bonds disappear. However, the symmetric stretching vibration of $-SO_3$ groups still remain. Due to the chemical structural and apparent degradation of MB17 after 90 min, it can be concluded that the degradation was mainly caused by breaking N=N bonds.

In photodegradation, dyes are usually degraded by free radicals generated from photocatalysts [24]. Electron paramagnetic resonance (EPR) was applied to examine the radical generation. Four common active species related to oxygen, including superoxide radical ($\cdot O_2^-$), hydroxyl radical ($\cdot OH$), singlet oxygen ($^1O_2$) and hole (h^+), were investigated at room temperature in air. 5,5-dimethyl-1-pyrroline N-oxide (DMPO) was employed as the spin trap of $\cdot O_2^-$, $\cdot OH$ and h^+, while 2,2,6,6-tetramethylpiperidinooxy (TEMPO) was used to capture $^1O_2$. As shown in Fig. 2b, the characteristic 1:2:2:1 peaks corresponding to the $\cdot OH$ adduct can be observed in the aqueous solution, so are the other 3 different kinds of signals. Therefore, we can conclude that all the radicals are generated by TpBD under visible-light irradiation.

To figure out which radical is mainly responsible for the photocatalytic degradation, different trapping agents were added into the mixture of TpBD and MB17 aqueous solution. 1 mmol L^{-1} of 1,4-benzoquinone (BQ), tert-Butanol (tB), ethylenediaminetetraacetic acid disodium salt (EDTA-2Na) and TEMPO were employed as scavengers to quench $\cdot O_2^-$, $\cdot OH$, h^+ and $^1O_2$, respectively. As shown in Fig. 2c, without any scavenger, MB17 could be photocatalytic degraded 90.3% by TpBD in 90 min. However, when scavengers added, degradation efficiency was conspicuously influenced. Compared to the MB17 solution with only TpBD, addition of tB, TEMPO and EDTA-2Na caused less degradation, 76.2%, 79.1% and 69.5% respectively, falling by 14.1%, 11.2% and 20.8%. However, when adding BQ into the MB17 solution, significant change happened. The concentration of MB17 solution remained, and no degradation could be observed, indicating that BQ caused complete catalyst deactivation of TpBD. From the result of scavenger test, we understand that $\cdot OH$, h^+ and $^1O_2$ have less contribution, while $\cdot O_2^-$ is the main contributor for the photocatalytic degradation of dyes under visible light.

Based on above observations, a possible photocatalytic degradation mechanism (Fig. 2d) can be proposed. When photon energy from illumination is greater than or equal to the

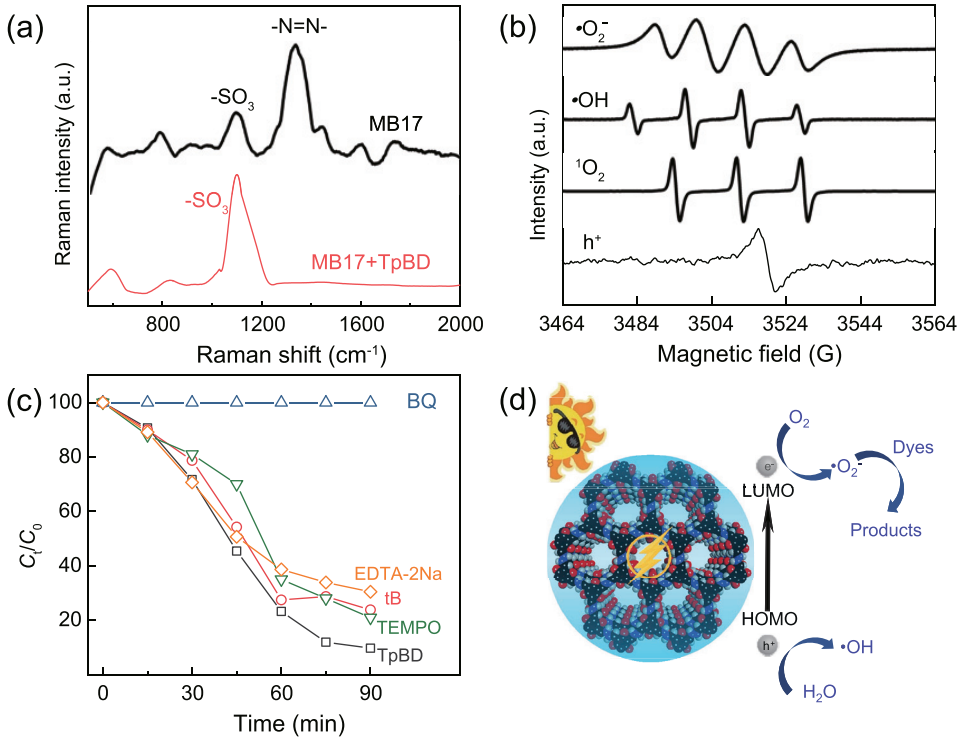

Fig. 2. (a) Raman spectra of MB17 and degradation product of MB17 photocatalytic degraded by TpBD. (b) EPR of O_2^-, OH, h^+ and $^1O_2$ in water with TpBD under visible-light irradiation. (c) Effects of scavengers on degradation of MB17. (d) Mechanism of the photocatalytic degradation by using COFs as catalysts.

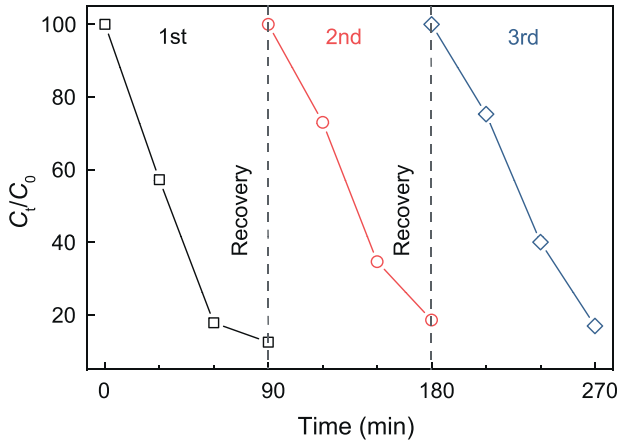

Fig. 3. Recyclability of TpBD in the photocatalytic degradation of MB17.

E_g of COFs (2.19 eV for TpBD), electron–hole pairs are generated. Superfluous photo-induced electrons separate and migrate from valence band (VB) to conduction band (CB). Then enriched CB electrons can easily transfer to the surface of COFs and combine with dissolved oxygen to form active radicals. As the most efficient radical in this photocatalytic degradation, $\cdot O_2^-$ attacks the functional groups on the dye molecules, especially the chromophore N=N bonds. Then the chemical structure of the dyes collapses and the photocatalytic degradation is accomplished.

3.4. Recovery test

We studied the reusability of TpBD as a photocatalyst. After photocatalytic degradation, the TpBD and solution were separated by suction filtration processes. The TpBD in Buchner funnel was washing with 500 mL water and then dried in oven under 120 °C. It is worth noting that no color can be found in the eluent. After totally dried, the TpBD was collected and used as catalyst for next photocatalytic degradation test. There was almost no decay of the catalytic capacity in three cycles (Fig. 3). Without any other measures, the recycled TpBD could turn to initial state easily just by drying. After three times of visible-light photocatalytic degradation, TpBD lost only 4.47% of its degradation efficiency compared to the first time. We examine the morphology and XRD pattern of TpBD after reused for three cycles and no obvious changes can be found (Fig. S4). The peaks at 3.38° (corresponding to the regular channel structure) and 27.28° (representing π-conjugation between COF layers) showed no decline, meaning that TpBD can maintain its structure and keep good crystallinity during photocatalysis processes.

3.5. Photocatalytic generality of imine-linked COFs

We expect that other imine-linked COFs also have efficient photocatalytic degradation performance provided they have homologous structure and chemical composition to TpBD. Considering that TpPa has similar optical and electrical properties to TpBD, we then investigate the dye degradation capability of TpPa. According to the Tauc plot and extrapolated tangent line, E_g of TpPa was determined to 2.06 eV which was close to that of TpBD (Fig. 4a). We found that TpPa also exhibited excellent performance in the photodegradation of dyes, similar to that of TpBD. After 90 min of exposure to visible light, 87.7% of MB17, 82.0% of MB3, 71.8% of EBA, 62.6% of MR7 and 35.6% of EBT were degraded (Fig. 4b). The results suggest that other imine-linked COFs with regular 2D π-conjugation structures should also have high efficiency in photocatalytic degradation of azo dyes.

4. Conclusions

In summary, we discover that imine-linked COFs are efficient photocatalysts for visible-light degradation of azo dyes. It is found that these COFs degrade highly concentrated dyes under visible light within only 1 h thanks to their densely conjugated structure, large absorbance range, excellent dispersibility in water, and high surface area. Under visible light, COFs produce radicals like $\cdot O_2^-$, which attack N=N bonds in azo dyes, leading to the consequent degradation. Importantly, the COF photocatalysts can be repeatedly used without noticeable loss of degradation efficiency. This work not only demonstrates an efficient strategy to degrade synthetic dyes,

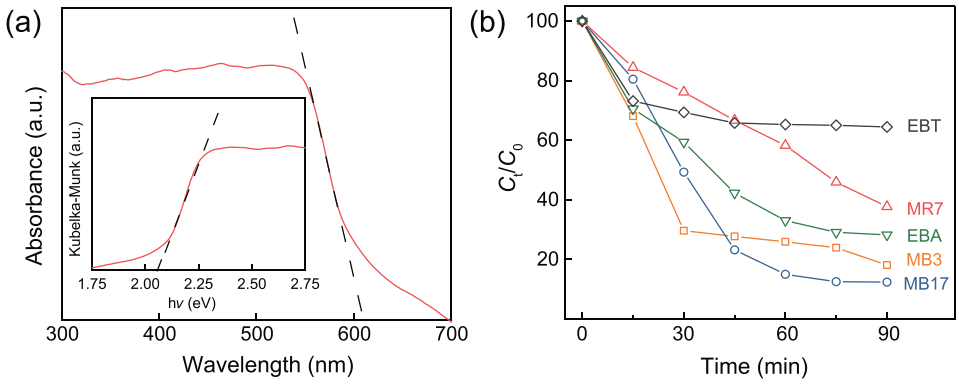

Fig. 4. (a) DRS spectrum of TpPa. Insert: E_g of TpPa determined by Kubelka–Munk function. (b) Photocatalytic degradation of dyes under visible-light irradiation with TpPa.

but also extends the application of emergent COFs to photocatalytic degradation.

Conflict of interest

There are no conflicts to declare.

Acknowledgements

This work was financially supported by the National Science Fund for Distinguished Young Scholars (21825803). We also thank the Program of Excellent Innovation Teams of Jiangsu Higher Education Institutions and the Project of Priority Academic Program Development of Jiangsu Higher Education Institutions (PAPD).

Appendix A. Supplementary data

Supplementary data to this article can be found online at https://doi.org/10.1016/j.gee.2020.09.010.

References

[1] S. Mondal, Environ. Eng. Sci. 25 (2008) 383–396.
[2] T.S.A. Singh, S.T. Ramesh, Environ. Eng. Sci. 30 (2013) 333–349.
[3] D.A. Yaseen, M. Scholz, Int. J. Environ. Sci. Technol. 16 (2019) 1193–1226.
[4] T. Robinson, G. McMullan, R. Marchant, P. Nigam, Bioresour. Technol. 77 (2001) 247–255.
[5] Y.L. Pang, A.Z. Abdullah, Clean 41 (2013) 751–764.
[6] Y.B. Zhou, J. Lu, Y. Zhou, Y.D. Liu, Environ. Pollut. 252 (2019) 352–365.
[7] T. Ngulube, J.R. Gumbo, V. Masindi, A. Maity, J. Environ. Manag. 191 (2017) 35–57.
[8] S.T. Ong, P.S. Keng, W.N. Lee, S.T. Ha, Y.T. Hung, Water 3 (2011) 157–176.
[9] M. Solis, A. Solis, H.I. Perez, N. Manjarrez, M. Flores, Process Biochem. 47 (2012) 1723–1748.
[10] H. Tong, S.X. Ouyang, Y.P. Bi, N. Umezawa, M. Oshikiri, J.H. Ye, Adv. Mater. 24 (2012) 229–251.
[11] I.K. Konstantinou, T.A. Albanis, Appl. Catal. B Environ. 49 (2004) 1–14.
[12] M. Stylidi, D.I. Kondarides, X.E. Verykios, Appl. Catal. B Environ. 47 (2004) 189–201.
[13] T.X. Wu, G.M. Liu, J.C. Zhao, H. Hidaka, N. Serpone, New J. Chem. 24 (2000) 93–98.
[14] S. Kaur, V. Singh, Ultrason. Sonochem. 14 (2007) 531–537.
[15] S. Yagi, Y. Fujie, Y. Hyodo, H. Nakazumi, Dyes Pigm. 52 (2002) 245–252.
[16] M.S. Masoud, H.H. Hammud, H. Beidas, Thermochim. Acta 381 (2002) 119–131.
[17] A. Afkhami, L. Khalafi, Supramol. Chem. 20 (2008) 579–586.
[18] J.Y. Zhang, J.A. Yang, H. Gao, Z.X. Du, T.M. Wang, Catal. Commun. 16 (2011) 175–179.
[19] J.L. Segura, M.J. Mancheno, F. Zamora, Chem. Soc. Rev. 45 (2016) 5635–5671.
[20] R.R. Liang, X. Zhao, Org. Chem. Front. 5 (2018) 3341–3356.
[21] W. Zhao, L.Y. Xia, X.K. Liu, CrystEngComm 20 (2018) 1613–1634.
[22] C.L. Tan, X.H. Cao, X.J. Wu, Q.Y. He, J. Yang, X. Zhang, J.Z. Chen, W. Zhao, S.K. Han, G.H. Nam, M. Sindoro, H. Zhang, Chem. Rev. 117 (2017) 6225–6331.
[23] M. Bhadra, S. Kandambeth, M.K. Sahoo, M. Addicoat, E. Balaraman, R. Banerjee, J. Am. Chem. Soc. 141 (2019) 6152–6156.
[24] Y.H. Fu, X.L. Zhu, L. Huang, X.C. Zhang, F.M. Zhang, W.D. Zhu, Appl. Catal. B Environ. 239 (2018) 46–51.
[25] P. Pachfule, A. Acharjya, J. Roeser, T. Langenhahn, M. Schwarze, R. Schomacker, A. Thomas, J. Schmidt, J. Am. Chem. Soc. 140 (2018) 1423–1427.
[26] R. Wang, X.S. Shi, A.K. Xiao, W. Zhou, Y. Wang, J. Membr. Sci. 566 (2018) 197–204.
[27] S. Chandra, S. Kandambeth, B.P. Biswal, B. Lukose, S.M. Kunjir, M. Chaudhary, R. Babarao, T. Heine, R. Banerjee, J. Am. Chem. Soc. 135 (2013) 17853–17861.
[28] B.P. Biswal, S. Chandra, S. Kandambeth, B. Lukose, T. Heine, R. Banerjeet, J. Am. Chem. Soc. 135 (2013) 5328–5331.
[29] Z. Liang, X. Bai, P. Hao, Y. Guo, Y. Xue, J. Tian, H. Cui, Appl. Catal. B Environ. 243 (2019) 711–720.
[30] F.-M. Zhang, J.-L. Sheng, Z.-D. Yang, X.-J. Sun, H.-L. Tang, M. Lu, H. Dong, F.-C. Shen, J. Liu, Y.-Q. Lan, Angew. Chem. Int. Ed. 57 (2018) 12106–12110.
[31] N. Xu, R.L. Wang, D.P. Li, X. Meng, J.L. Mu, Z.Y. Zhou, Z.M. Su, Dalton Trans. 47 (2018) 4191–4197.